BJRS

BRAZILIAN JOURNAL
OF
RADIATION SCIENCES
07-03A (2019) 01-12

Monitoring internal contamination from Occupationally Exposed Workers of an ^{18}F-FDG production plant: Whole Body Counter or Head Counting setup?

Mendes[a] B.M., Trindade[b] B.M., Fonseca[c] T.C.F., Campos[c] T.P.R.

[a] *Centro de Desenvolvimento da Tecnologia Nuclear – CDTN/CNEN*
Av. Presidente Antônio Carlos, 6.627 31270-901 Belo Horizonte, MG
[b] *University of Ottawa. Ottawa, Ontario, Canada*
[c] *Universidade Federal de Minas Gerais – UFMG*
bmm@cdtn.br

ABSTRACT

The production ^{18}F-FDG for positron emission tomography (PET) has consistently increased over the past two decades. The risk of internal contamination at ^{18}F-FDG production facilities exists. A setup for evaluation of the ^{18}F-FDG activity incorporated into the occupationally exposed workers brain, called Head Counting System (HCS), was presented in previous works. In this study, the whole body counter setup (WBC) was evaluated for monitoring ^{18}F incorporations. The Monte Carlo Virtual Software (VMC in-vivo) and the MCNPx code were used to assess the system calibration coefficient (CC). Three ^{18}F distributions were simulated: i) uniformly distributed in soft tissue (UDST); ii) Na^{18}F biodistribution (NAFB); and iii) ^{18}F-FDG biodistribution (FDGB). The calibration coefficient of WBC was compared to the current head counting system CC under the same biodistribution conditions. The ICRP male reference voxelized phantom was used in the simulations. The results showed that the WBC setup was more efficient than the head counter for all the studied ^{18}F distributions: UDST = 1060 %, FDGB = 488 % and NAFB = 340 %. Despite this, especially for ^{18}F-FDG, the possibility of bladder voiding before measurement can lead to considerable uncertainties when the WBC setup is used. On the other hand, bladder activity does not show great influence the calibration coefficient of the head counting system. Future work will evaluate the WBC sources of uncertainties in the measurement of ^{18}F incorporated activity.

Keywords: Internal Dosimetry, MCNPx, VMC in-vivo, ^{18}F-FDG incorporation.

ISSN: 2319-0612
Accepted: 2019-04-01

1. INTRODUCTION

The production of PET radiopharmaceuticals has increased considerably in recent years [1]. The most widely used PET radiopharmaceutical in the world continues to be fludeoxyglucose F 18 (^{18}F-FDG) [2]. Images with ^{18}F-FDG have been used in the diagnosis, staging, prognosis and evaluation of therapeutic efficacy for several types of cancer [2].

Despite the increased risk of internal contamination, due to the intensification and dissemination of ^{18}F-FDG production, few studies have addressed this issue [1], [3]–[6]. Typically, ^{18}F-FDG synthesis take place in sealed hot cells and it is highly automated. Nevertheless, internal contaminations of the occupationally exposed workers (OEW) during production processes have already been reported [1], [5]. The possible contaminants in ^{18}F-FDG synthesis are fluoride ions ($^{18}F^-$), fluoromethane ($CH_3{}^{18}F$) [1] and ^{18}F-FDG itself [5]. The first two can lead to internal contamination by inhalation [1] and the last one by ingestion or inhalation [5].

In vitro and *in vivo* monitoring techniques can be used to estimate radioactive intakes from ^{18}F-FDG synthesis [3], [6]. Environmental air monitoring can also provide good estimates of the incorporated activity [3]. Oliveira et al., (2012) developed an *in vivo* setup for the quantification of ^{18}F-FDG uptakes based on the measurement of the activity accumulated in the brain [5]. It was called Head Counting System (HCS) On the other hand, Calandrino et al., (2009) chose Whole Body Counters (WBC), lung counters and *in vitro* techniques to estimate the incorporated activity from ^{18}F-FDG synthesis contaminants [3].

The aim of this work was to evaluate if WBC is more effective than HCS to detect and quantify internal contaminations from ^{18}F-FDG production. Simulations using the Monte Carlo MCNPx and Monte Carlo Virtual Software (VMC in-vivo) codes were performed for this purpose.

2. MATERIALS AND METHODS

The Monte Carlo codes, MCNPx, version 2.7.0, [7] and VMC in-vivo, compiled 02/02/2016, [8]–[10] were used to simulate two counting geometries. The whole body counter geometry uses an 8" x 4" NaI(Tl) detector positioned between the thorax and the abdomen, as can be seen in Figure 1.

A 3” x 3” NaI(Tl) detector was positioned facing the top of the head for the Head Counting System (HCS) geometry (Figure 1). The details of the MCNPx simulations of 3” x 3” NaI(Tl) detector are shown in Figure 2. The 8” x 4” detector was simulated with the same components except the MgO reflector. The dimensions were set according its size. The Phantoms and the detectors were positioned inside an air sphere with 250 cm radius.

Figure 1: *Counting geometries evaluated. The WBC uses an 8” x 4” NaI (Tl) detector and the HCS uses a 3” x 3” NaI (Tl) detector. A) MCNPx plot mode of the simulation geometry. B) Adapted picture showing the VMC geometries. C) Details of the simulation of 3” x 3” NaI(Tl) detector.*

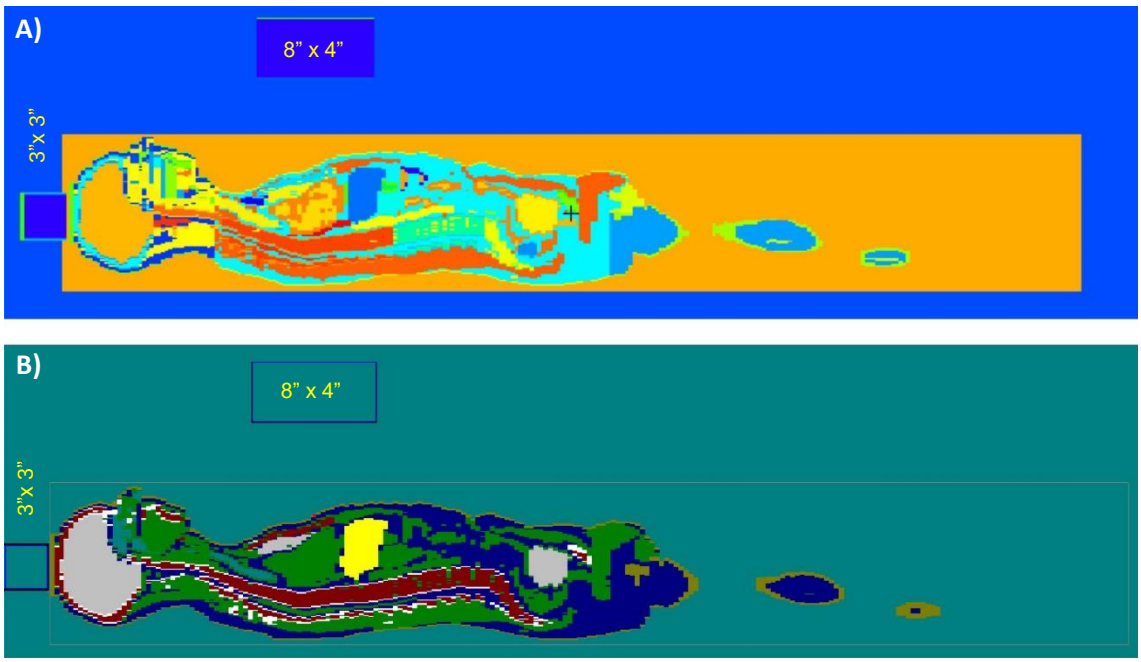

Source: Author’s archive.

In MCNPx simulations, the following structures were represented in the NaI(Tl) detectors: NaI(Tl) crystal, aluminum wall, aluminum window, MgO reflector and photomultiplier tube (PMT) glass window. The composition of the detector materials and dimensions were based in literature data and in the equipment manuals [15, 16]. Elemental composition, in weight percentage (w%),

and density (g.cm^3) of the detector structures are shown in Table 1. VMC in-vivo simulations used the <IRD 8" x 4".txt> and < 3 x 3 IRD NaI.txt> detector files.

Figure 2: *Picture detailing the simulation of 3" x 3" NaI(Tl) detector structures. The NaI(Tl) crystal, Magnesium oxide reflector, Aluminum wall and window and the photomultiplier tube window can be observed.*

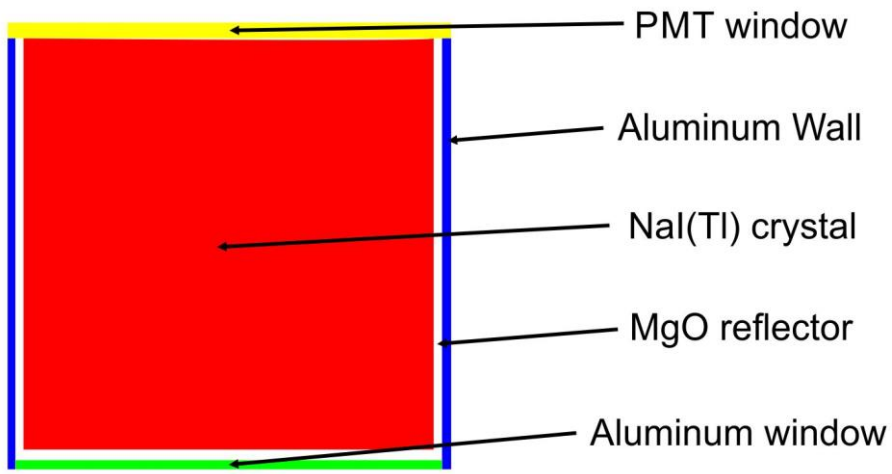

Source: Author's archive.

Table 1: Elemental composition (w%) and density (g.cm^3) of the NaI(Tl) detector structures according to the literature [15, 16].

Element	Elemental composition of the Detector components (w%)			
	NaI Crystal	Aluminum Wall and window	MgO reflector	PMT window
O	-	-	39.70	53.26
Na	15.34	-	-	-
Mg	-	-	60.30	-
Al	-	100	-	-
Si	-	-	-	46.74
I	84.66	-	-	-
ρ (g.cm^3)	3.667	2.7	2.0	0.94

The ICRP reference male voxelized phantom, RCP_AM, was used in the simulations [11]. This is an adult male reference phantom with 176 cm height and 73 kg. The voxels dimensions are (2.137 x 2.137 x 8.0 mm^3) and the matrix is (256 x 129 x 224) voxels. Tissue compositions and densities were also based in ICRP 110 publication [11]. Three types of biodistribution of the ^{18}F radioisotope were simulated in MCNPx: i) uniformly distributed in soft tissue (UDST); ii) $Na^{18}F$ biodistribution (NAFB); and iii) ^{18}F-FDG biodistribution (FDGB). The representation of the three biodistributions proposed are shown in Figure 3.

Figure 3: *Representation of the three biodistributions proposed in this study. A) $Na^{18}F$ biodistribution (NAFB). B) ^{18}F-FDG biodistribution (FDGB). C) Fluoromethane ($CH_3{}^{18}F$) uniformly distributed in soft tissue (UDST).*

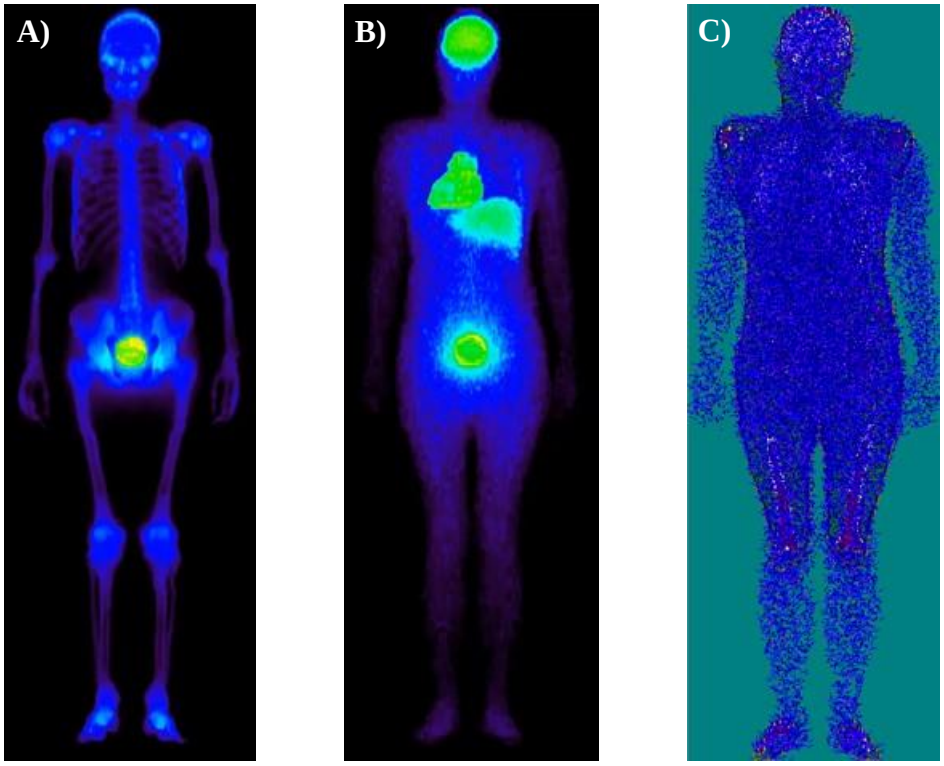

Source: Author's archive.

As the fluoromethane ($CH_3{}^{18}F$) biodistribution was not found in literature, it was considered uniformly distributed in the soft tissues of the body. ICRP 128 present current information about

biokinetic data for major radiopharmaceuticals [12]. The fluoride ions ($^{18}F^-$) biodistribution reflected the $Na^{18}F$ radiopharmaceutical biodistribution found in ICRP 128 [12]. ^{18}F-FDG distribution on the body tissues was also found in ICRP 128 [12]. The radiopharmaceuticals biodistribution data were based in intravenous injection so they are valid for inhalation and ingestion only if the bioabsorption is very fast. Data from Calandrino et al., (2009) suggests that this assumption is true for fluoride ions [3]. However, data about ^{18}F-FDG bioabsorption in the lung or in the gastrointestinal tract were not found. Only ^{18}F uniformly distributed in soft tissue (UDST) was simulated with VMC in-vivo because that is the only biodistribution pattern direct available. The obtaining calibration coefficients for the other biodistribution patterns involving different uptake in organs (NAFB or FDGB) is not impossible with VMC in-vivo, but requires more refined calculations or code changes, which is not the objective of using VMC in this work.

Positron sources distributed in the organs\regions determined by biodistribution data were simulated. ICRP publication 133 recommendations were taken in to account for particle emissions from source organs [13]. Energy *versus* probability table for ^{18}F positron emissions was provided by the DECDATA® software [14]. The cutoff energy for photons and electrons was 1 keV (default). Secondary particle transport was taken into account (mode p e). Energy distribution of the photon pulses occurring in the sensitive volumes of NaI(Tl) detectors was assessed with tally F8:p [7]. The pulses were tallied in energy bins, incremented by 1.0 keV (0-2000 keV). The number of positrons stories followed (NPS) was set to 1.0E+07 for MCNPx and VMC in-vivo simulations. 120 cores of the cluster Orion of the Laboratório de Metrologia de Nêutrons on Instituto de Radioproteção e Dosimetria (LN/IRD), with 37 AMD Phenom(tm) II X6 1100T processors, 16 GB de memory each, were used for MCNPx simulations. VMC in-vivo simulations were made in a PC with an Intel® Core™ i7-5500U, 2.4 GHz CPU and 8 GB memory.

The Calibration Coefficient ($CPS \cdot Bq^{-1}$) was calculated from MCNPx simulations according to equation 1, as follows:

$$CC = 0.9673 \cdot PPPos \quad (1)$$

where 0.9673 is the number of positrons emitted per ^{18}F decay [14], PPPos is the number of 511 keV photon pulses in the sensible volumes of NaI(Tl) detectors per positron emitted from the source.

VMC in-vivo is easier to use and was designed to simulate counting systems geometry, thus it present the Calibration Coefficient value directly and no further calculation is required.

3. RESULTS AND DISCUSSION

The computational times for cases simulated on the MCNPx, ranged from 2 to 6 hours per case. The relative errors at 511 keV peaks were less than 1%. The energy spectra per positron emitted on the source for WBC and HCS geometry and considering the ^{18}F uniformly distributed in the soft tissues are shown in Figure 4. The photopeak can be identified in 511 keV, the Compton edge in 340 keV, and the backscatter peak in 170 keV. The iodine scape peak can also be observed at 482 keV. Still in Figure 4, it can be noted that, mainly for the energy range below the photopeak, the points are more dispersed in the curve referring to the head counter than for the whole body counter one. This occurs because of the worse statistics for the energy bins of HCS geometry. Since the same number of particles histories were followed for the two geometries studied, this indicates that WBC geometry is more efficient. To reduce the relative error of the channels below the photopeak of the HCS geometry, a simple solution, but computationally costly, would be to increase the NPS to 1.5E+08. This should result in relative errors of the same order of magnitude as those obtained for the WBC geometry. However, the focus of this work is to evaluate the efficiency of photopeak and the relative errors in this energy bin are sufficiently low (< 1%).

The results of the calibration coefficients obtained using MCNPx and VMC in-vivo, for the different biodistribution conditions and geometries were presented in Table 2. It was observed a good correlation between MCNPx and VMC in-vivo results. The counting efficiency was higher for the whole body counter than for the head counter in all biodistribution conditions. The higher percent ratio between WBC/HCS calibration coefficients was observed for UDST biodistribution (>1000% for MCNPx and VMC in-vivo). Even for the lower percent ratio, for the NAFB biodistribution, the WBC geometry was three times more efficient. It should be noted that the detector used in WBC geometry is larger than the one used in HCS geometry. Since the same number of particles was simulated for the two different geometries, the most efficient geometry

(WBC) should present better counting statistics, i.e., smaller relative errors and standard deviations. HCS geometry using an 8" x 4" NaI(Tl) detector should be evaluated in the future.

Figure 4: *MCNPx energy distribution of the photon pulses occurring in the sensitive volumes of NaI(Tl) detectors considering the WBC geometry (orange) and the HCS geometry (blue), for ^{18}F uniformly distributed in the soft tissues. The 511 keV photopeak (PP), the iodine scape peak (EP), the Compton edge (CE) and the backscattered peak (BSP) can be located in the spectrum.*

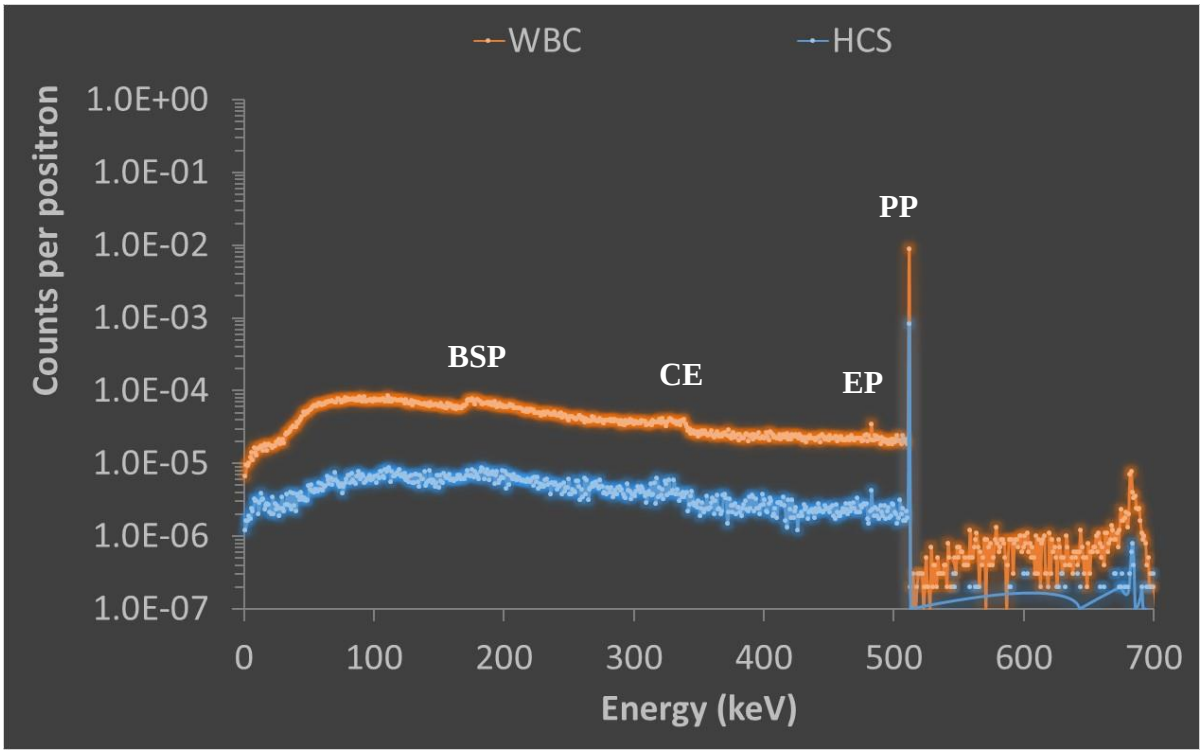

Source: Author's archive.

The counting efficiency is an important factor to be considered when choosing a counting geometry to *in vivo* monitoring of internal contaminations. However, it is not the only one. For example, in the cases of ^{18}F-FDG and Na^{18}F, the bladder is the organ where the highest number of decays occur [12]. In another work not published yet, we found that the calibration factors for decays occurring only in urinary bladder are 3.50E-03 ± 0.06E-03 Cps.Bq^{-1} for the WBC and 2E-06 ± 1E-06 Cps.Bq^{-1} for the HCS. Taking in to account the biodistribution data from ICRP 128 [12],

i.e., 10.4% and 14.5% of the decays occur in the bladder for ^{18}F-FDG and Na^{18}F respectively, the difference in calibration factors if the bladder is empty should be -4.4 % for ^{18}F-FDG and -9.4 % for Na^{18}F for the WBC geometry. These values are -0.1 % for ^{18}F-FDG and -0.2 % for Na^{18}F for the HCS geometry. Considering that ICRP 128 data provide mean values, the percentage of the decays in urinary bladder could vary considerably as a function of time. In this way the differences in CC should be higher than ones previous mentioned. Thus, if the bladder is empty just before the *in vivo* monitoring, the efficiency may fall and underestimations could occur. Emptying of the bladder introduces smaller uncertainties for the head counter geometry. In this way, the simultaneous use of WBC an HCS geometry should be very useful, taking benefits of the best characteristics of both systems.

Table 2: Calibration coefficients for the different biodistribution conditions and geometries, obtained using MCNP and VMC in-vivo.

Biodistribution / MC Code	**Head Counter (HCS)**		**Whole Body Counter (WBC)**		**% Ratio WBC/HCS[c]**
	CC[a] (CPS.Bq^{-1})	**SD[b](CPS.Bq^{-1})**	**CC[a] (CPS.Bq^{-1})**	**SD[b](CPS.Bq^{-1})**	
FDGB / MCNPx	1.786E-03	1.322E-05	8.710E-03	2.874E-05	488 %
NAFB / MCNPx	1.745E-03	1.291E-05	5.939E-03	2.376E-05	304 %
UDST / MCNPx	7.969E-04	8.765E-06	8.445E-03	2.871E-05	1060 %
UDST / VMC in-vivo	7.937E-04	9.76E-06	8.340E-03	1.729E-04	1026 %

[a] - CC = Calibration coefficients; [b] - SD = Standard deviation (SD = Mean value · Relative Error);
[c] - % Ratio WBC/HCS = (CC_{WBC} / CC_{HCS}) · 100.

Another option would be to request the OEW to empty the bladder prior to *in vivo* monitoring. In this case, the CC without bladder activity should be obtained and the uncertainties would decrease, especially in the case of the WBC geometry. However, a decrease of 4% to 10% (or even higher) in counting efficiency would also be expected depending on the biodistribution of ^{18}F.

4. CONCLUSION

The simulations performed were very useful to evaluate two counting geometries for *in vivo* monitoring of possible internal contaminations in an ^{18}F-FDG production plant.

Results from VMC in-vivo simulations showed good correlation with MCNP results, proving one more time the usefulness of this free MC code.

Whenever possible, the WBC and the HCS geometries should be used simultaneously for OEW contamination monitoring, since the first has higher counting efficiency and the second is less sensible to urinary bladder voiding uncertainties. If only WBC geometry is available, the empty the bladder procedure should be adopted prior the monitoring.

ACKNOWLEDGMENT

We would like to thank the Neutron Metrology Laboratory of the Institute of Radioprotection and Dosimetry (IRD/CNEN) for allowing the use of the Orion high-performance cluster to perform the MCNPx simulations. The following Brazilian institutions supported this research project: Fundação de Amparo à Pesquisa de Minas Gerais (FAPEMIG), e Conselho Nacional de Desenvolvimento Científico e Tecnológico (CNPq).

REFERENCES

[1] CALANDRINO, R.; DEL VECCHIO, A.; TODDE, S.; FAZIO, F. Measurement and control of the air contamination generated in a medical cyclotron facility for PET radiopharmaceuticals. **Health Phys**, v. 92(5 SUPPL. 2), p. S70-S77, 2007.

[2] SHARMA, P.; MUKHERJEE, A. Newer positron emission tomography radiopharmaceuticals for radiotherapy planning: an overview.," **Ann Transl Med**, v. 4(3), p. 1-7, 2016. http://dx.doi.org/10.3978/j.issn.2305-5839.2016.01.26

[3] CALANDRINO, R.; DEL VECCHIO, A.; SAVI, A.; TODDE, S.; BELLOLI, S. Intake risk and dose evaluation methods for workers in radiochemistry labs of a medical cyclotron facility. **Health Phys**, v. 97(4), p. 315-321, 2009.

[4] CALANDRINO, R.; DEL VECCHIO, A.; PARISI, R.; TODDE, S.; DE FELICE, P.; SAVI, A.; PEPE, A.; MRSKOVA, A. Measurements and evaluation of the risks due to external radiation exposures and to intake of activated elements for operational staff engaged in the maintenance of medical cyclotrons. **Radiat Prot Dosimetry**, v. 139(4), p. 477–482, 2010.

[5] OLIVEIRA, C.M.; LIMA, F.F.; OLIVEIRA, M.L.; SILVA, T.V.; DANTAS, A.L.; DANTAS, B.M.; ALONSO, T.; SILVA, T.A. Evaluation of a technique for in vivo internal monitoring of18f within a Brazilian Laboratory Network. **Radiat Prot Dosimetry**, v. 153(1), p. 100-105, 2013.

[6] OLIVEIRA, C.M.; SILVA, T.V.; ALONSO, T.C.; DANTAS, B.M.; DANTAS, L.A.; SILVA, T.A. Validação da Metodologia para Monitoração Interna de Flúor-18 por meio da Unidade do Contador de Corpo Inteiro do CDTN, In: **XV CONGRESSO BRASILEIRO DE FÍSICA MÉDICA – CBFM**, 2010, Aracajú, Brasil, 2010, p. 1-5.

[7] PELOWITZ, D.B. **MCNPx User's Manual - Version 2.7.0**. Los Alamos National Laboratory report LA-CP-11-00438, April, 2011.

[8] HUNT, J.; DANTAS, B.; AZEREDO, A. Visual Monte Carlo and the Simulation of Whole Body Counter and Gamma Camera Counting Systems, In: **12th CONGRESS OF THE INTERNATIONAL RADIATION PROTECTION ASSOCIATION – IRPA 12**, 2008, Buenos Aires, Argentina, 2008, p. 1–4.

[9] HUNT, J.G.; DANTAS, B.M.; LOURENÇO, M.C.; AZEREDO, A.M.G. Voxel phantoms and Monte Carlo methods applied to in vivo measurements for simultaneous 241-Am contamination in four body regions. **Radiat Prot Dosimetry**, v. 105(1–4), p. 549-552, 2003.

[10] GÓMEZ-ROS, J.M.; DE CARLAN, L.; FRANCK, D.; GUALDRINID, LIS, M.; LÓPEZ, M.A.; MORALEDA, M.; ZANKL, M.; BADAL, A.; CAPELLO, K.; COWAN, P.; FERRARI, P.; HEIDE, B.; HENNIGER, J.; HOOLEY, V.; HUNT, J.; KINASE, S.; KRAMER, G.H.; LÖHNERT, D.; LUCAS, S.; NUTTENS, V.; PACKER, L.W.; REICHELT, U.; VRBA, T.; SEMPAU, J.; ZHANG, B. Monte Carlo modelling of Germanium detectors

for the measurement of low energy photons in internal dosimetry: Results of an international comparison. **Radiat Meas**, v. 43(2–6), p. 510-515, 2008.

[11] ICRP - International Commission on Radiological Protection. Adult Reference Computational Phantoms. ICRP Publication 110**. Ann ICRP**, v. 39(2), p. 21-45, 2009.

[12] ICRP - International Commission on Radiological Protection. Radiation Dose to Patients from Radiopharmaceuticals: a Compendium of Current Information Related to Frequently Used Substances. **Ann ICRP**, v. 44(2 Suppl), p. 7-321, 2015.

[13] ICRP - International Commission on Radiological Protection. The ICRP Computational Framework for Internal Dose Assessment for Reference Adults: Specific Absorbed Fractions. ICRP Publication 133. **Ann ICRP**, v. 45(2), p. 74, 2016.

[14] ICRP - International Commission on Radiological Protection. Nuclear decay data for dosimetric calculations. ICRP Publication 107. **Ann ICRP**, v. 38(3), p. 7-96, 2008.

[15] MOUHTI, I; ELANIQUE, A.; MESSOUS M.Y. Monte Carlo modelling of a NaI(Tl) scintillator detectors using MCNP simulation code. **J Mater Environ Sci**, v. 8(12), p. 4560-4565, 2017.

[16] SALGADO, C.M.; BRANDÃO, L.E.B.; SCHIRRU, R.; PEREIRA, C.M.N.A.; CONTI, C.C. Validation of a NaI(Tl) detector's model developed with MCNP-X code. **Prog Nucl Energ**, v. 59, p. 19-25, 2012.